8th Symposium on Fire and Forest Meteorology
13-15 October 2009, Kalispell, MT-USA

NUMERICAL SIMULATION OF THE INTERACTION BETWEEN TWO FIRE FRONTS IN THE CONTEXT OF SUPPRESSION FIRE OPERATIONS

Dominique Morvan[(1)], Chad Hoffman[(2)], Francisco Rego[(3)], William Mell[(4)]

(1) Laboratoire de Mécanique, Modélisation et Procédés Propres (M2P2)
UNIMECA Université d'Aix-Marseille
Technopôle de Château Gombert 60 rue Joliot Curie
13453 Marseille cedex 13 France, Email : dominique.morvan@univmed.fr
(2) Department of Forest Resources College of Natural Resources
University of Idaho Moscow ID-USA
(3) ISA-CEABN Tapada da Ajuda 1349-017 Lisbon Portugal
(4) BFRL-NIST 100 Bureau Drive, Gaithersburg MD-USA

Abstract

This paper deals with the study of physical phenomenon observed between two converging fire fronts (a head fire and a back fire), in conditions similar to those encountered during suppression fire operations. The simulations were carried out using two fully physical models (FIRESTAR, Wildland Urban Interface Fire Dynamics Simulator), including the resolution of the set of balance equations (mass, momentum, energy) governing the behaviour of the coupled system formed by the vegetation and the surrounding atmosphere. Two fuel profiles were tested: homogeneous grassland similar to landscapes in Australia and a shrubland representative of Mediterranean landscape (garrigue). The numerical results showed clearly how the two fire fronts interact together and mutually modify their own behaviour, before merging.

1. INTRODUCTION

To stop the propagation of a wildfire or reduce its intensity, fire fighters rely on reducing one side of the fire triangle: fuel, heat and air. In an unconfined configuration and for a fully developed fire, it is difficult to directly affect the air supplying the fire front. Consequently, fire fighters focus their efforts to reduce the heat released by the fire, using water or foam, or to eliminate the fuel located between the fire front and the control line. The reduction of fuel can be accomplished using mechanical means (bulldozer) or by using a suppression fire (also called counter fire or back fire), which is a traditional technique of fire fighting (Chandler et. al 1983). During the last decades this technique was reintroduced as an alternative tool when classical terrestrial or aerial means were non-operational or not sufficiently efficient. As indicated by Goldammer and De Ronde (2004), one can formally distinguish two techniques: burnout operations and backfiring operations. Burnout operations use techniques very similar to prescribed burning with the goal to burn the vegetation located between the main fire and the control line. The use of suppression fire is more aggressive and consists of igniting a fireline as close as possible to the main fire front. In this case, it is expected that the main fire front will generate an in-draft flow which facilitates the propagation of the back fire. Both fire fronts propagate in opposite directions before merging. The back fire, having burned all the available solid fuel ahead of the main fire front, blocks the progression of and rapidly extinguishes the wildfire; see Chandler & al (1983), Goldammer and De Ronde (2004), Pyne & al (1996).

* Corresponding Author Address: Dominique Morvan, Laboratoire de Mécanique, Modélisation et Procédés Propres (M2P2) UNIMECA Université d'Aix-MarseilleTechnopôle de Château Gombert 60 rue Joliot Curie 13453 Marseille cedex 13 France, Email : dominique.morvan@univmed.fr

Very few studies have been published on this subject; for example, it is not well known at what distance (as the function of the fireline intensity) a wildfire can interact with a back fire (in-draft distance).

Pitts (1991) examined interactions between wind and fires, focusing on how multiple fires interact and eventually merge. Depending on burner distribution, this experimental study showed that the fuel consumption rate reached a maximal value, then decreased because of the limitation on air supply causing by adjacent burners. More recently, Roxburgh and Rein (2008) performed numerical simulations using Fire Dynamics Simulator (FDS developed by the Building and Fire Research Laboratory BFRL-NIST), to study the in-draft flow generated ahead of a wildfire by the convection plume. In this study, the fire was represented as a fixed burner, using a wide range of fire intensity (from 1 to 10 MW/m) and wind speed velocity (from 1 to 15 m/s). Considering the behaviour of the flow field ahead of the fire front, the authors distinguished three zones: Zone 1 is nearest the fire front where the wind field was directly affected by flame dynamics, Zone 2 is located at the maximum furthest distance from the main fire front at which a backing fire is influenced by the winds from the main fire front, and Zone 3 is located at a distance from the main fire front such that the behaviour of the backing fire is dominated by external atmospheric flow. They present numerical results highlighting the extension of the Zone 2 as a function of the fire intensity. The results also indicated that the maximum distance from the main fire front where a back fire can benefit from the in-draft flow ranged from 15 m to 70 m. In addition to numerical simulations, a set of experimental fires were conducted to study the conditions of success of suppression fires, as part of the EU FP6 Program FIREPARADOX. These experiments were conducted in Mediterranean mixed heathland (fuel depth ranged between 40 and 60 cm, fuel load from 1.5 to 2.5

kg/m^2), for relatively moderate wind conditions (average wind velocity less than 6 m/s). The experiments showed clearly that the air flow was significantly affected by the fire fronts. For moderately high wind velocity conditions (4 m/s), back fire kept a rate of spread (ROS) almost constant (~0.02 m/s). After a short period of acceleration, following the ignition, the head fire reached a quasi-steady state (ROS~0.33 m/s). When the distance separating the two fire fronts was equal to 20 m, the head fire accelerated suddenly (ROS~0.63 m/s). For moderate wind conditions (1 m/s), for the back fire and the head fire propagated with a ROS equal to 0.03 m/s (back fire) and 0.25 m/s (head fire) respectively. Just before the collision the progression of the two fire fronts was accelerated to 0.45 m/s (back fire) and 0.61 m/s (head fire). In this case, the in-draft flow, ahead of the main fire, modified the behaviour of the back fire, which became a secondary head fire. For these conditions, the interaction distance between the two fire fronts was equal to 70 m (Vega et al., 2008). We can conclude after this first set of experiments that it is not so easy to define the ideal situation to ignite a suppression fire; as it was observed in the experiments, some conditions favourable for the entrainment of the back fire toward the head fire (in-draft flow) also considerably modified the ROS of the back fire, increasing its intensity and degrading the safety of fire fighters.

It was the goal of this project to investigate the usefulness and ability for physics-based simulation methods to capture the general behaviour reported in the field experiments. We further anticipate that the results of these types of simulations may lead to the development of better guidelines for the use of back fires and also provide additional research hypothesis.

2. PHYSICAL MODEL

For this study, the propagation of fire through two fuel layers was simulated. This approach utilized two fully physical models: one using a two dimensional formulation (FIRESTAR) and the other using a three dimensional formulation (Wildland Urban Interface Fire Dynamics Simulator, or WFDS). Both of these approaches include the main physical mechanisms, initially proposed by Grishin (1996), governing the behaviour of the coupled system formed by the vegetation and the surrounding atmospheric flow. The heterogeneous structure of the vegetation is taken into account using a set of solid fuel families which represent the fine fuels (thickness smaller than 6 mm) contributing directly to the propagation of the fire, namely foliage, branches and twigs. Fuel elements submitted to intense heat transfer by convection and radiation coming from the flame are dehydrated and decomposed (pyrolysis process) into gas (mainly CO and CO_2) and solid (charcoal) products within the simulations. The gaseous combustion in the flame is calculated assuming that the reaction rate was mainly limited by the turbulent mixing between the gaseous pyrolysis products and the ambient air (eddy dissipation combustion model). Both radiative and convective heat transfer between the flame (soot-gas mixing) and the vegetation is included. The interaction between the atmospheric boundary layer flow and the vegetation layer is also taken into account in the simulations, by adding volume drag force terms in the equations governing the turbulent fluid flow (momentum, turbulent kinetics energy, turbulent dissipation rate). See Morvan et al (2004, 2009) for a detailed description of FIRESTAR model and Mell et al (2007) for a detailed description of the WFDS model. The FIRESTAR model was developed during the European project FIRESTAR and FIREPARADOX (6th & 7th EU Framework Program) and was intensively tested on various conditions in grassland, Mediterranean shrubland and boreal forest (Morvan & al, 2004, 2009) and compared with data collected during campaigns of experimental fires (see Cheney & al (1993), Fernandes (2001) and Stocks et al (2004)).

3. NUMERICAL RESULTS AND DISCUSSION

A first set of simulations was carried out in 2D using FIRESTAR, for a uniform fuel layer, using similar conditions to experimental campaigns performed in grassland in Australia (Cheney et al, 1993) (the physical properties were summarized in table 1). To sustain the propagation of the back fire, mainly governed by radiation heat transfer, the mesh size is the streamwise δ_X and the vertical direction δ_Z was chosen such that $\delta_X = 2\ \delta_R$ and $\delta_Z = \delta_R /2$, where δ_R designed the extinction length scale (equal to 0.24 m for this particular case). To represent accurately turbulent structures induced by shearing effect above the vegetation layer, we also imposed that δ_Z verified the following constrain $\delta_Z < H_{FUEL} / 4$. To restrain the propagation of the two fire fronts (main fire and back fire), the fuel was distributed between two points along the streamwise direction: X=10 and X=110 m (see Figure 1). Assuming that the initial velocity profile (on the left end side of the computational domain) was logarithmic before to be eventually affected by the presence of the fire, the calculations were performed for 3 values of the 10m open wind velocity U_{10} equal to 1.3 , 2.6 and 5.2 m/s (see Figure 1). To stabilize the initial air flow conditions, the flow was computed during the first 20s without any source of energy, then, two burners were activated simultaneously to ignite the fuel at the two end points. The temperature field and the velocity vectors of the gaseous phase obtained for a wind speed U_2 equal to 2 m/s (U_{10} = 2.6 m/s) are shown in Figure 2. These 3 snapshots (obtained 68 s, 78 s and 82 s after the ignition of the fuel) are representative of the three main steps observed during a suppression fire operation:

1) The free propagation in opposite directions of the two fire fronts (the main fire on the left and the back fire on the right) converging toward the same meeting point
2) The phase during which the two fire fronts can interact, just before their merging
3) The merging of the two fire fronts in a single fire

For these relatively moderate wind conditions, our results indicate that the rate of spread (ROS) characterizing the main fire (ROS=0.71 m/s) was a little bit larger than the values observed for the back fire (ROS=0.54 m/s), however, it was not as large as was expected. This could be due to the particular propagation regime induced for moderate wind conditions, as well as the fuel moisture regime used (FMC=6%). In this case, the air flow in the vicinity of

the two fire fronts was greatly affected by the fire itself, reducing in the same way the influence of the wind flow, and the propagation of both head fire and back fire was mainly governed by the radiation heat transfer between the flame and the unburned vegetation located ahead of the fire front. The total (head fire + back fire) fireline intensity was equal to 5999 kW/m and was nearly equal to the sum of fire intensities calculated in simulating the head fire and the back fire separately, for which we found a value equal to 5691 kW/m. The time history of the temperature (Figure 3) calculated for two points located 0.5m above the ground level, at X=60m (P1) and X=80m (P2), on both side of the meeting point of the two fires (~X=68m), allowed to highlighted also the differences in behaviour of the two fire fronts. At the first point (P1), we can see the travelling of the main fire front, characterized by a sharp increased of the temperature signal, the maximum temperature calculated at this point was nearly equal to 1440 K, we evaluated that the fire residence time (τ) of the head fire was equal to 13 s. At the second point (P2) (affected by the travelling of the back fire), the temperature signal was more extended in time, the fire residence time was multiply by a factor 3.5 (τ = 46 s) and the temperature reached a maximal value sensibly smaller than for the head fire, equal to 840 K.

The values of the ROS obtained for 3 values of the 10m open wind velocity U_{10}, were reported in Figure 4 for calculations simulating a suppression fire operation (FIRESTAR head fire & back fire) and compared with results obtained for a single fire propagating along the wind direction (FIRESTAR AU Grass). The results were also compared with experimental data collected during experimental fires and bushfires in similar conditions (Cheney & al, 1993). We also added the predictions obtained using empirical (MK5) or semi-empirical operational (BEHAVE) models.

These results showed that, as indicated previously, in these conditions, except during the short time before the merging of the two fire fronts, the propagation of the head fire was not significantly affected by the presence of the back fire; the ROS with and without the back fire were sensibly the same (see Figure 4). We also noticed that the ROS associated with the back fire was weakly affected by the wind flow; this result was not surprising, considering that the back fire was isolated from the action of the wind flow by the presence of the head fire and that the propagation of the back fire was mainly piloted by the radiation heat transfer between the flame (pushed on the leeward side) and the unburned vegetation.

This set of simulations was also conducted with FIRESTAR in a more complex fuel layer, representing a Mediterranean shrubland. The fuel complex containing two species (*Quercus coccifera* and *Brachypodium ramosum*), was represented using 4 families of solid fuel elements (see Table 2) contributing directly to the propagation of the fire. We tested 5 values of the 10m open wind velocities (U_{10}), ranging between 2 and 16 m/s. In all simulations, these conditions led to a sustained propagation for the head fire and the back fire, with the exception of 2 m/s and 16 m/s for which we noticed a more or less rapid extinction of the back fire.

The results in Figure 5 show the temperature field calculated 20 s and 85 s after the ignition of the two fires, for a wind speed U_{10} equal to 4 m/s. Comparing the two temperature fields, we noticed a sudden increase of the flame height during the merging phase between the two fires (see also Figure 6). Such a sudden event is often reported by fire fighters and foresters during suppression fire operations. It could be attributed to an accumulation of pyrolysis products between the two fire fronts. Just before the meeting of the two fires, the mutual interaction between the two fires could be forming pockets of unburned pyrolysis products, which suddenly ignited at the end of the operation. The conditions contributing to the development of this sudden modification of the fire dynamics is not fully understood at this moment. Additional studies are needed in order to improve the safety conditions of people leading suppression fire operations. The interaction between the two fire fronts is quite complex, and it cannot be summarized by the in-draft flow generated under some circumstances by the main front. This interaction can be also greatly affected by the wind flow conditions and the fuel load, as shown in Figure 7. The conditions of propagation and the effectiveness of the back fire can be greatly affected by the trajectory of the plume of the main fire.

In addition to the two-dimensional numerical simulation using FIRESTAR, we conducted two numerical simulations in three dimensions using the boundary fuel method in the Wildland Urban Interface Fire Dynamics Simulator version 4 (Mell et al., 2007). These simulations were set up using 11 computational meshes spanning a total of 1500 x 1500 x 200 meters in the x, y and z dimensions respectively. The fuel bed was positioned in the center mesh (300 x 300 x 200 m) as a 100 x 100 m plot. Consequently, the interactions between firefronts was equal to that of the FIRESTAR simulations. A 30-m wide strip of fuel with the same properties as listed in Table 1 was located around the border of the fuel plot but was not allowed to burn. The grid resolution within the center mesh was set as 1.66 m in the x and z direction and stretched from 1.38 m near the ground to 5.5 m at 200 m above the ground. All other meshes had the same grid resolution in the z dimension and a 3.33 m resolution in the x and y dimensions. This configuration is similar to that used in Mell et al. (2007). The wind flow in the simulation was initially defined throughout the domain as $U = U_2 (z / 2)1/7$, $V = W = 0$, where U_2 is the wind at a height of 2 m. The wind speed at 2 m was set at 2 m/s (U_2 = 2 m/s). A total of two simulations were conducted using WFDS, the first was a head fire-only simulation and the second was a simulation which included both a head fire and backing fire. Fires were ignited instantaneously along a 100 m line for the head fire and back fire scenario and along a 100 m line for the head fire only scenario.

Rate of spread of head fire-only simulations are higher than those previously reported for WFDS simulations in similar fuel beds and environmental conditions and the empirical values reported in Australian grass fire experiments (Cheney et al 1997) (Figure 8). The

difference between these simulations and the experimental values and previous simulations could in part be caused by differences in the spatial domain of the burning area (200 x 200 m in past WFDS simulations and in the AU experiments and 100 x 100 m in this study). When both the head fire and back fire are ignited we see an overall decrease in the head fire rate of spread compared to the head fire only case (Figure 9). Figure 10 shows the two simulations at 83 s after ignition; from these images it is clear that in the head and back fire scenario there is a reduction in the head fire rate of spread. When viewed over time both the head fire and backing fire initially show a period of time with increasing fire rate of spread followed by a period of time with a more constant fire rate of spread, and finally a period of time in which the rate of spread was highly variable. This final period characterized by high variability in rate of spread seems to start at about 50 s after ignition occurred (Figure 9). This phenomenon appears to be a result of the two fire fronts interacting.

The heat release rate of the two scenarios (Figure 11) suggests that, outside of the initial build-up period, the two fires behave fairly similarly until the two fires come together at about 85 s into the simulation (a spike in the heat release rate is evident Figure 11). Conversion of total heat release rate to fireline intensities suggests that fireline intensities varied from about 4000 to 4500 kw/m during the steady state period of time for both the head fire only and for the head fire and back fire simulations. During the merging of the two fire fronts we see a spike in the fireline intensity which reaches a maximum value of 5900 kw/m.

Comparisons of the average rate of spread values obtained from both FIRESTAR and WFDS for the head fire (~0.7 m/s) and the back fire (~0.4 m/s) in the two fire front simulations were in a relative agreement with each other. Both models also tend to show three clear phases in the interaction of fire fronts: first, the free propagation in opposite directions of the two fire fronts (the main fire on the left and the back fire on the right) converging toward the same meeting point; second, a phase during which the two fire fronts interact; and third, the merging of the two fire fronts into a single fire. In both simulations the merger of the two fire fronts occurred around 83 s after ignition. These results suggest that the two simulation approaches used in this study are behaving similarly to each other despite the additional complexity introduced by the third dimension. However, some flow from the sides of the fire front. These flow effects are not possible to simulate in a 2-diminsional environment and may explain why the WFDS simulations report a reduction in head fire rate of spread for two fire fronts while the FIRSTAR simulations do not. The inclusion of this flow pattern also explains why the average head fire rate of spread for the single fire front simulation is higher in WFDS. In addition, the fireline intensities simulated using FIRESTAR are on average over 1500 kw/m higher compared to the WFDS simulated fireline intensities. more general discrepancies between the two simulation approaches were identified through this study. In particular, comparisons of the 3-dimensional WFDS simulations suggest that the reduction of head fire rate of spread occurring when a second fire front is added may be caused by the reduction of incoming air

4. CONCLUSION

Suppression fire operations were simulated using two fully physical models, in simplified configurations, on a flat terrain, for two types of vegetation layer: Australian grassland and Mediterranean shrubland. The two approaches used in this study both show clear signs of three distinct phases of interaction between two fire fronts in a suppression fire. First, a stage of free propagation in opposite directions of the two fire fronts; secondly, a phase during which the two fire fronts interact; and finally, the merging of the two fire fronts into a single fire. Both simulation approaches also suggest that the merging of the two fire fronts results in a quick increase in fireline intensity. This sudden event constitutes a potential source of danger for people present during these operations. The results showed also that the behaviour of the back fire, and consequently its effectiveness, can be greatly affected by the trajectory of the plume of the main front. Therefore, the efforts to understand the complex physical phenomena occurring during a suppression fire operation must continue. Specifically, we need 1) further 3-D simulation approaches which investigate how the length of ignition of the back fire affects these interactions, and 2) 2- and 3-D simulations which investigate the effectiveness of suppression fires for more complex fuel beds and different wind speeds. We also need to further investigate scenarios in which the head fire is already fully developed at the time of suppression fire ignition. In addition to further simulation work, there is a real need for experimental research involving the interaction of two fire fronts. In particular, we need more data on the change in flow associated with fire front interactions for different fireline lengths; greater initial separation of head and back fires; presence of flanking fires, various ambient wind speeds needs to be investigated further as well as the effects of this flow. Such projects would be useful to allow for the evaluation and improvement of simulation methods and for the development of empirical rules of thumb that could be useful for fire operations personnel.

5. REFERENCES

Chandler, C., Cheney, Ph., Thomas, P., Trabaud, L. 1983: Fire in forestry, Vol.1 & 2, John Wiley & Sons.

Cheney, N.P., Gould, J.S., Catchpole, W.R. 1993: The influence of fuel, weather and fire shape variables on fire spread in grasslands. *Int. J. Wildland Fire,* 3(1), 31-44.

Fernandes, P.A.M. 2001: Fire spread prediction in shrub fuels in Portugal. *Forest Ecology & Management*, 144, 67-74.

FIREPARADOX: http://www.fireparadox.org/

Goldammer, J.G., De Ronde, C. 2004: Wildfire fire management handbook for sub-Sahara Africa, Global Fire Monitoring Center (GFMC).

Grishin, A.M. 1996: Mathematical modelling of forest fires and new methods of fighting them. Albini F. (Ed.) Tomsk State University.

Mell W., Jenkins M.A., Gould J., Cheney Ph. 2007. A physics-based approach to modelling grassland fires. *Int. J. Wildland Fire,* 16, 1

Morvan, D. 2009: Some physical phenomena contributing to the behaviour of wildfires. Proceedings of 6th International Symposium on Turbulence, Heat & Mass Transfer, Rome (Italy), 14-18 September 2009.

Morvan, D., Dupuy, J.L. 2004: Modelling the propagation of a wildfire through a Mediterranean shrub using a multiphase formulation. *Combustion & Flame*, 138, 199-200.

Morvan, D., Méradji, S., Accary, G. 2009: Physical modelling of fire spread in Grasslands. *Fire Safety Journal*, 44, 50-61.

Pitts, W.M. 1991: Wind effects on fires. *Prog. Energy Combust. Sci.*, 17, 83-134.

Pyne, S.J., Andrew, P.L., Laven, R.D. 1996: Introduction to wildland fire, John Wiley & Sons, 2nd Edition.

Roxburgh, R., Rein, G. 2008: Study of wildfire in-draft flows for counter fire operations. *Proceedings of Forest Fire 2008, International Conference on Modelling, Monitoring and Management of Forest Fires, Toledo, Spain,* 10p.

Stocks, B.J., Alexander, M.E., Wotton, B.M., Stefner, C.N., Flannigan, M.D., Taylor, S.W., Lavoie, N., Mason, J.A., Hartley, G.R., Maffey, M.E., Dalrymple, G.N., Blake, T.W., Cruz, M.G., Lanoville, R.A. 2004: Crown fire behaviour in a northern jack pine – black spruce forest. *Canadian J. Forest Research.* 34, 1548-1560.

Vega, J.A., Jiménez, E., Pérez, J.R. 2008: Effectiveness of suppression fires: methods and first results. Deliverable D2.3-2 of the IP FIREPARADOX (FP6-018505), European Commission, 27p.

Table 1: Physical properties characterizing the fuel layer used for the calculation performed in grassland.

Fuel density (kg/m^3)	514
Fuel packing ratio x 10^3	1.36
Fuel moisture content (%)	6
Fuel depth (m)	0.5
Surface area to volume ratio (m^{-1})	12240
Leaf area index (LAI)	4.16

Table 2: Physical properties characterizing the fuel layer used for the calculation performed in shrubland.

	Leaves	Twigs (0-2mm)	Twigs (2-6mm)	Grass
Fuel density (kg/m^3)	810	900	930	440
Fuel packing ratio (average) x 10^3	2.175	1.15	2.175	1
Fuel moisture content (%)	30	30	30	5
Fuel depth (m)	0.75	0.75	0.75	0.25
Surface area to volume ratio (m^{-1})	5920	2700	1000	20000
Leaf area index (LAI)			6.00	

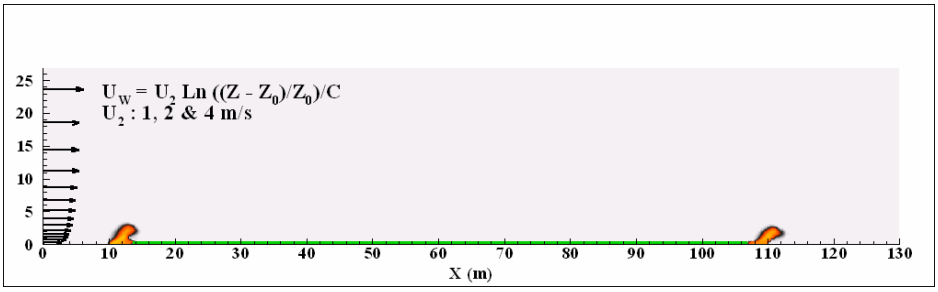

Figure 1: Interaction between two fire fronts in grassland: geometry and wind velocity profile imposed at the inlet of the computational domain.

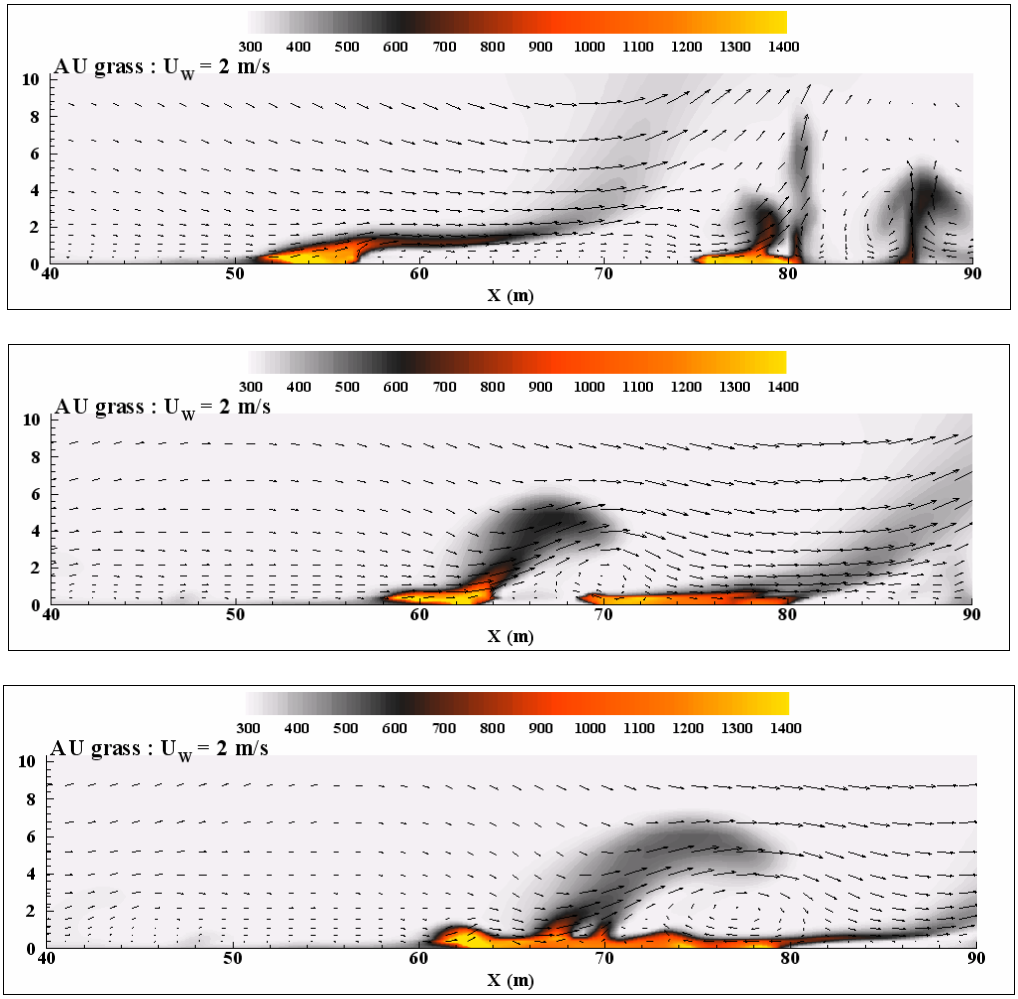

Figure 2: Temperature and velocity vectors calculated during the propagation of a head (on the left) and a back fire (on the right) in a grassland 68 s, 78 s and 82 s after the simultaneous ignition of the two fires and for a wind speed U_2 equal to 2 m/s (U_{10}=2.6 m/s).

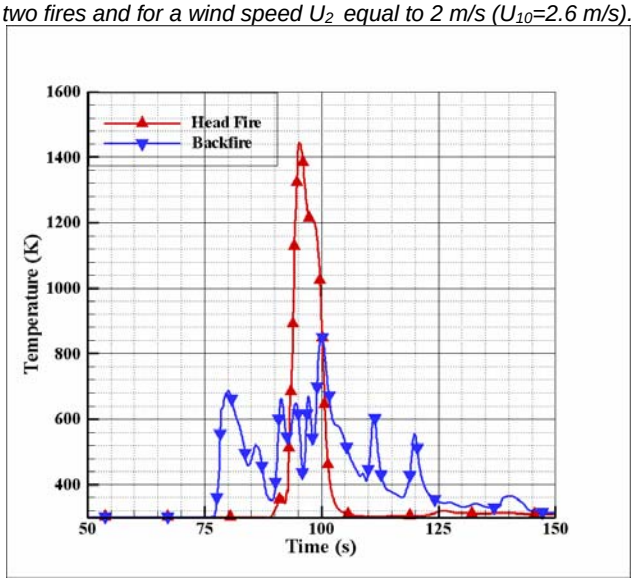

Figure 3: Temperature time history for two points located at X=60m and X=80m respectively affected by the arrival of the head fire and the back fire (U_2=2 m/s).

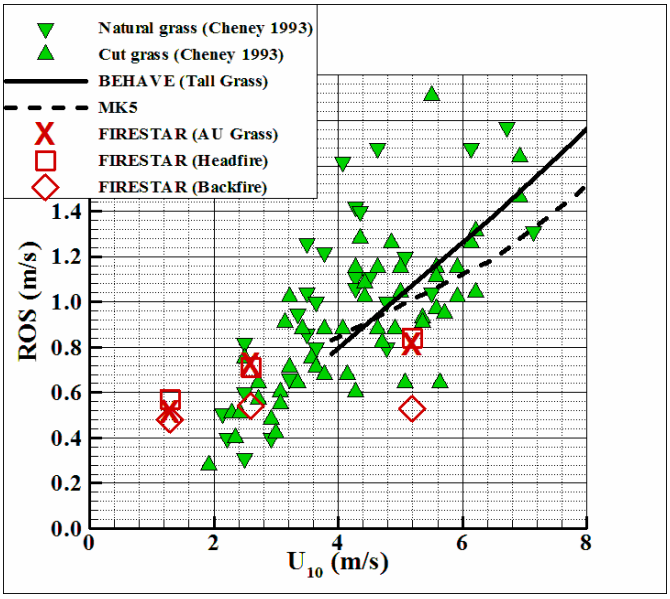

Figure 4: Rate of spread (ROS) versus 10m open wind speed (U_{10}) of the head fire and the back fire compared with the values during the propagation of a single surface fire by simulation (FIRESTAR AU Grass) and experimentally (Cheney & al 1993).

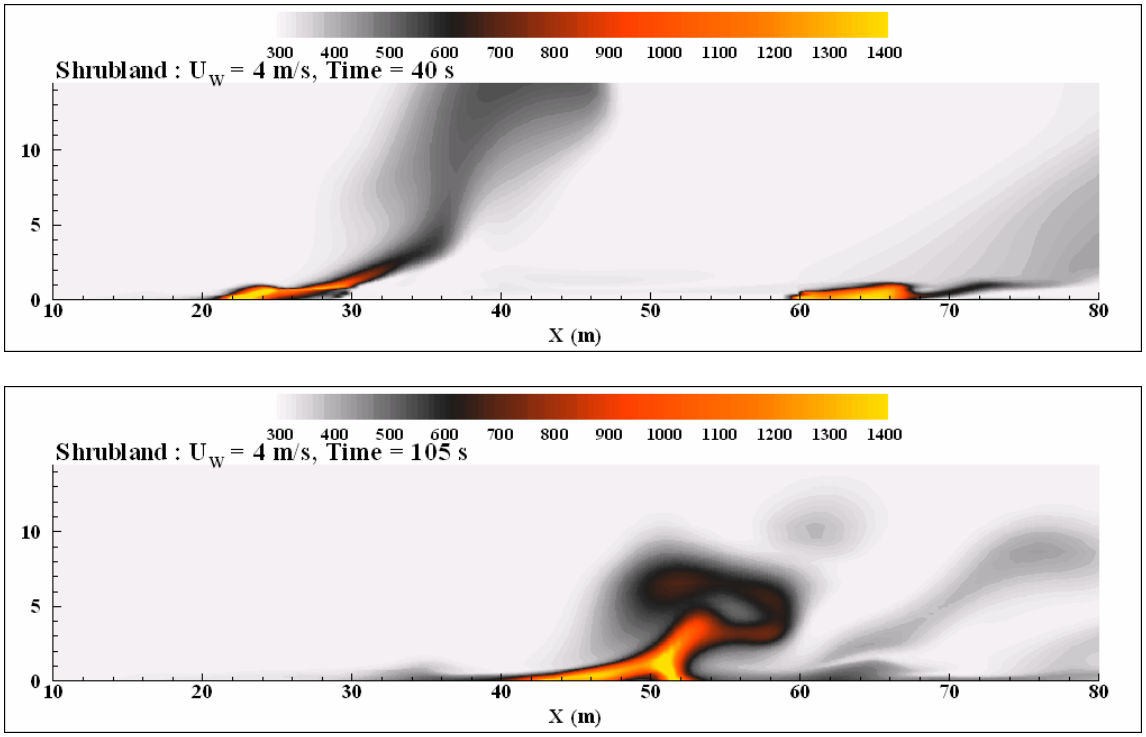

Figure 5: Temperature field calculated during a suppression fire operation carried out in a Mediterranean shrubland 20 s and 85 s after the simultaneous ignition of the two fires and for a wind speed U_{10} equal to 4 m/s.

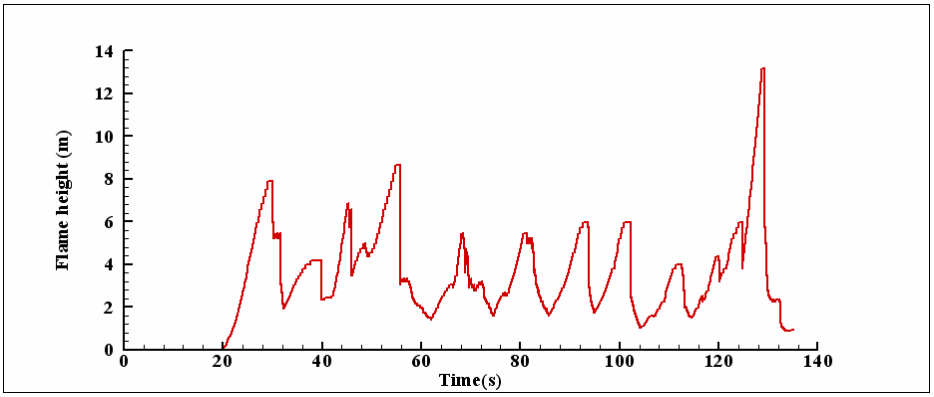

Figure 6: Time evolution of the flame height (isotherm T = 700 K) during a suppression fire simulation in a Mediterranean shrubland (U_{10} = 4 m/s).

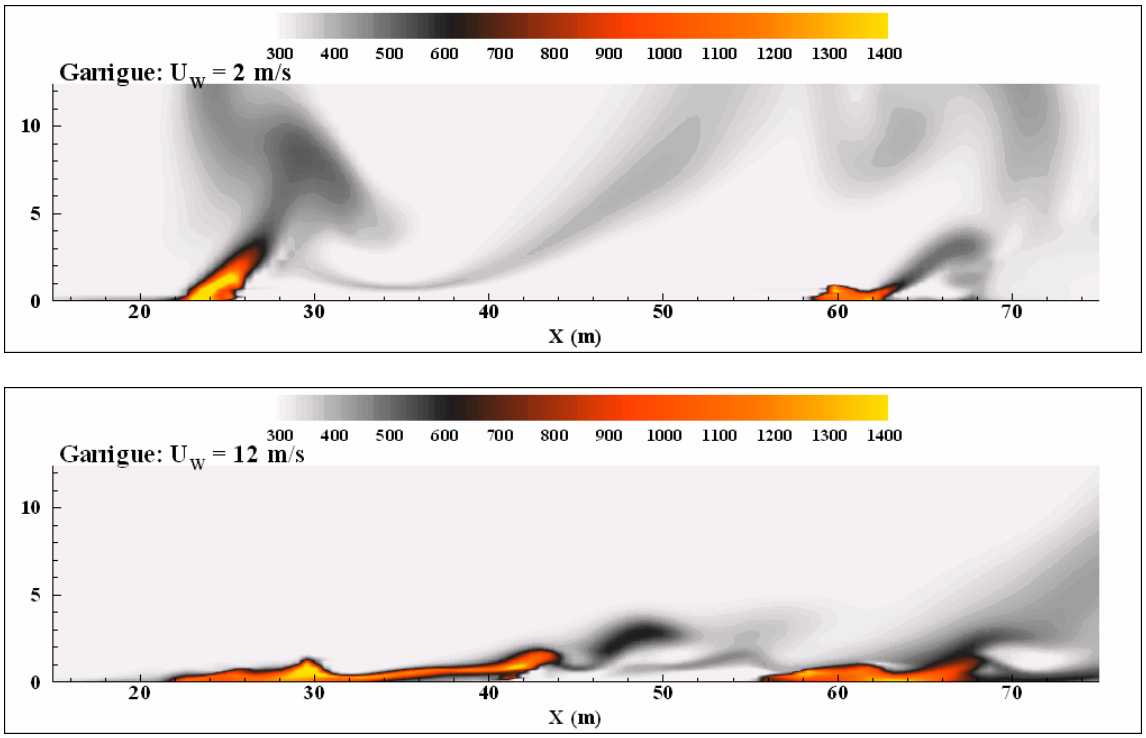

Figure 7: Temperature field calculated during a suppression fire operation carried out, in a Mediterranean shrubland for two wind speed U_{10} equal to 2 m/s (top) and 12 m/s (bottom).

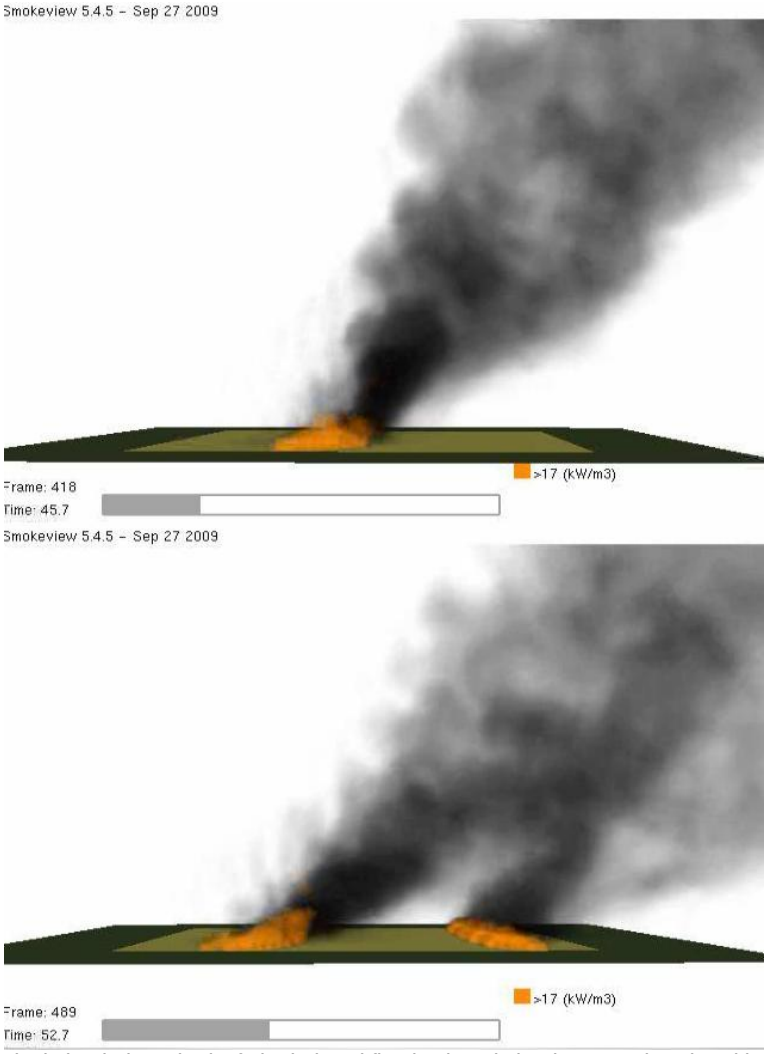

Figure 8: Numerical simulations (3D) of single head fire (top) and simultaneous head and back fire (bottom) propagating in grassland for a wind speed velocity U_2 = 2 m/s.

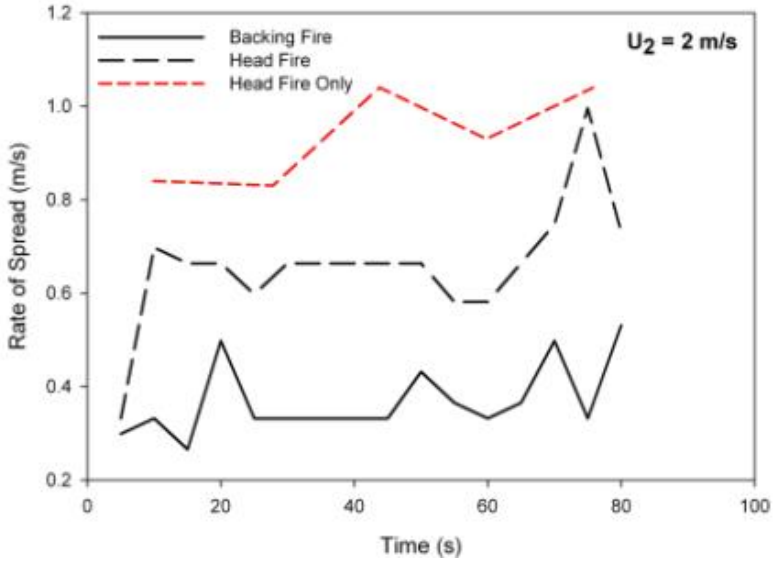

Figure 9: Rate of spread (ROS) evaluated during 3D simulations of single head fire and simultaneous head and back fire in grassland.

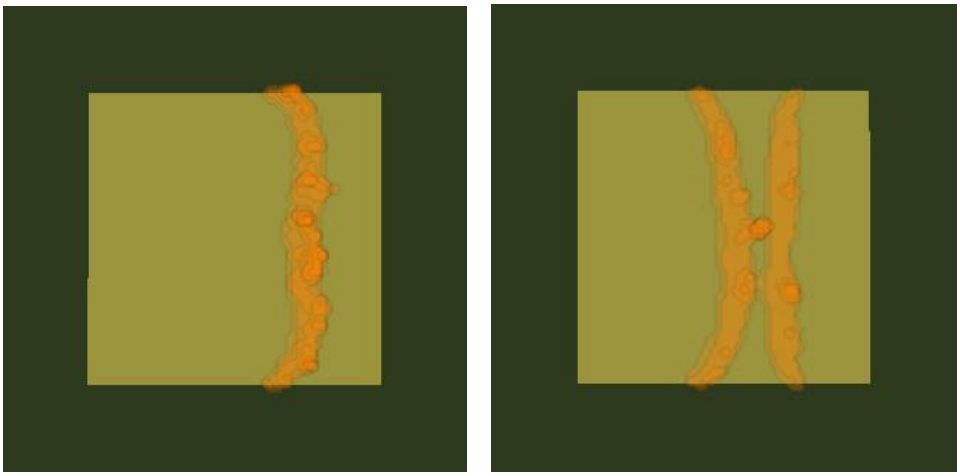

Figure 10: Top view of the fire fronts 83 s after the ignition: single head fire (left), head and back fire (right).

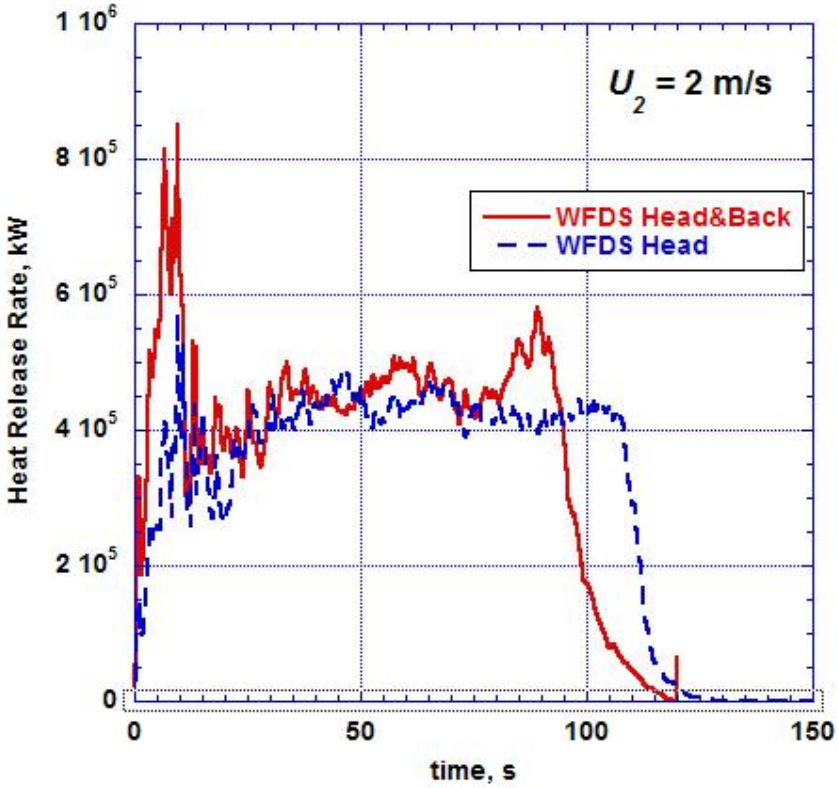

Figure 11: Time evolution of the heat release rate calculated in 3D using WFDS.